Diffusive transport and self-consistent dynamics in coupled maps

Guido Boffetta,[1] Diego del-Castillo-Negrete,[2] Cristóbal López,[3] Giuseppe Pucacco,[4] and Angelo Vulpiani[5]

[1]*Dipartimento di Fisica Generale and INFM, Università di Torino, via P. Giuria 1, 10125 Torino, Italy*
[2]*Oak Ridge National Laboratory, Oak Ridge, Tennessee 37831-8071*
[3] *Dipartimento di Fisica, Università di Roma La Sapienza, P.le A. Moro 2, 00185 Roma, Italy*
[4]*Dipartimento di Fisica, Università di Roma Tor Vergata, via della Ricerca Scientifica 1, 00133 Roma, Italy*
[5]*Dipartimento di Fisica and INFM UdR and SMC Center, Università di Roma La Sapienza, p.le A. Moro 2, 00185 Roma, Italy*

The study of diffusion in Hamiltonian systems has been a problem of interest for a number of years. In this paper we explore the influence of self-consistency on the diffusion properties of systems described by coupled symplectic maps. Self-consistency, i.e., the backinfluence of the transported quantity on the velocity field of the driving flow, despite of its critical importance, is usually overlooked in the description of realistic systems, for example, in plasma physics. We propose a class of self-consistent models consisting of an ensemble of maps globally coupled through a mean field. Depending on the kind of coupling, two different general types of self-consistent maps are considered: maps coupled to the field only through the phase, and fully coupled maps, i.e., through the phase and the amplitude of the external field. The analogies and differences of the diffusion properties of these two kinds of maps are discussed in detail.

I. INTRODUCTION

Understanding transport is a problem of considerable practical and theoretical interest in a great variety of fields ranging from geophysics to chemical engineering and plasma physics. In some situations one can safely consider the simple case of *passive transport* in which the transported quantity does not affect the advecting flow [1,2]. In the case of a scalar passive field $\Theta(\mathbf{x},t)$, the evolution equation is the advection-diffusion equation

$$\frac{\partial \Theta}{\partial t} + \mathbf{\nabla} \cdot (\mathbf{v}\Theta) = D_0 \nabla^2 \Theta, \qquad (1)$$

where $\mathbf{v}(\mathbf{x},t)$ is the velocity field, D_0 the molecular diffusivity, and Θ represents the scalar concentration, e.g., the temperature of the fluid or the concentration of a pollutant. The domain of applicability of Eq. (1) is limited by two important physical assumptions: Θ has to be *inert* (no possible chemical or biological reactions are considered) and passive (there is no feedback on the velocity). Reactive processes can be taken into account by adding to the right hand side of Eq. (1) a function $f(\Theta)$ modeling the reaction kinetics [3]. This leads to the so-called advection-reaction-diffusion equations widely used in the modeling of chemical and biological systems including combustion, diluted chemical reactions, and population dynamics [4].

Taking into account the feedback of Θ on $\mathbf{v}$, i.e., the problem of *active transport*, is in general more complicated as this involves the equation of motion for $\mathbf{v}$. Because of this, active transport is also called *self-consistent transport*. A well-known example is fluid convection in the Boussinesq approximation [5]. In this case, Θ represents the fluid temperature, which is an active scalar in the sense that it modifies the velocity field through the buoyancy force in the Navier-Stokes equation for $\mathbf{v}$.

The goal of the present paper is to study the problem of diffusion of active scalars. In particular, we are interested in the relationship between self-consistent chaos and diffusion due to chaotic advection. The study of diffusion requires an accurate numerical integration of the equations of motion for very long times and many initial conditions. A common strategy to bypass this technical difficulty is to describe the time-continuous equations of motion with a discrete-time map. Here we follow this approach and study the problem of diffusion in self-consistent symplectic maps. In the remaining of this introduction we discuss in some detail the problem of self-consistent transport in fluids and plasmas. The intent of this discussion is to provide a physical motivation for the use of globally coupled maps for studying self-consistent transport.

One of the simplest physical examples of active transport is two-dimensional incompressible flows. This motion is described by Navier-Stokes equation (1) in which Θ represents the vorticity, $\zeta = \mathbf{\nabla} \times \mathbf{v}$. Plasma physics is another area in which the problem of self-consistent transport is crucial. For example, in the Vlasov description of an electron plasma [6] (in a uniform neutralizing ion background) the system is described by the phase space electron distribution function f which, for an one-dimensional system, evolves according to the Liouville equation

$$\partial_t f + u\partial_x f + \partial_x \phi \partial_u f = D_0 \partial_u^2 f, \qquad (2)$$

where the term on the right hand side is a Fokker-Planck collision operator, and (x,u) are the phase space coordinates. This equation is analogous to Eq. (1) if one identifies Θ with f, and $\mathbf{v}$ with the transport velocity in phase space $(u,\partial_x \phi)$. In this case the self-consistent coupling is provided by the Poisson equation

$$\partial_x^2 \phi = \int f(x,u,t)du - 1, \qquad (3)$$

where the right hand side is the charge distribution including the fixed neutralizing ion background. That is, the dynamics of an electron plasma is an active transport problem in which the transport velocity of the distribution function f in phase space is determined by f through Poisson's equation.

The previous ideas on self-consistent transport can be reformulated within the Lagrangian description according to which transport is described in terms of individual particle trajectories instead of scalar fields and distribution functions. The Lagrangian description is important because it is the natural description to formulate the self-consistent transport problem in terms of symplectic maps which are the main objects of study in the present paper. As it is well-known [7], the Lagrangian formulation of Eq. (1) is the Langevin equation

$$\frac{d\mathbf{x}}{dt} = \mathbf{v}(\mathbf{x},t) + \sqrt{2D_0}\,\boldsymbol{\eta}(t), \qquad (4)$$

describing the motion of a test particle (the tracer), where $\boldsymbol{\eta}$ is a normalized Gaussian white noise with zero mean and δ correlated in time:

$$\langle \eta_i(t)\eta_j(t')\rangle = \delta_{ij}\delta(t-t'). \qquad (5)$$

The passive scalar nature of Θ in Eq. (1) reflects in the absence of coupling in the Lagrangian equations of motion (4). However, in an active transport problem, the self-consistent coupling between the field and the transport velocity leads to a nonlinear coupling between the Lagrangian equations of motion. The fact that particles interact (and usually through long-range interaction) implies that the phase space evolution of particle n, depends on the position of all the N particles

$$\frac{d\mathbf{x}_n(t)}{dt} = \mathbf{v}(\mathbf{x}_1(t),\ldots,\mathbf{x}_N(t)), \qquad (6)$$

and therefore the system has a phase space of dimension proportional to N. This is the well-known N-body problem that arises in many fields of physics, including gravitational systems in Astronomy [8], point vortices in two-dimensional fluid dynamics [9], and atomic physics.

An approximation of the N-body problem (6), which is often used, is a mean-field type approximation in which the interaction among particles occurs through a global variable $\mathbf{X}$ function of all the particles. In the examples shown below, the mean field will depend on the mean distribution of particles only, thus Eq. (6) formally reduces to

$$\frac{d\mathbf{x}_n}{dt} = \mathbf{v}_{ext}(\mathbf{x}_n) + \mathbf{v}(\mathbf{x}_n - \mathbf{X}),$$

$$\frac{d\mathbf{X}}{dt} = \mathbf{F}(\mathbf{X},\{\mathbf{x}_k\}), \qquad (7)$$

where we have included the possible contribution of an external field $\mathbf{v}_{ext}$.

Recently, a mean-field description of this sort has been proposed to study self-consistent transport in fluids and plas-

mas [10–12]. In the plasma physics context, this approximation known as the single-wave-model (SWM), consists of simplifying the self-consistent coupling between f and ϕ given by Poisson's equation (3).

The SWM is a general model for the description of marginally stable fluids and plasmas [13,14]. Also the model bears many interesting analogies with coupled oscillator models used in statistical mechanics [15]. As such, it is an insightful model to explore the problem of self-consistent chaos, and will be our starting point for the construction of the self-consistent symplectic map models in the present paper.

The transition to the symplectic map description is eased by first writing the SWM as a full $N+1$ Hamiltonian system in the particle coordinates (x_j, u_j) and the mean field degrees of freedom [16,10]

$$\frac{dx_k}{dt} = \frac{\partial \mathcal{H}}{\partial p_k}, \quad \frac{dp_k}{dt} = -\frac{\partial \mathcal{H}}{\partial x_k}, \qquad (8)$$

$$\frac{d\theta}{dt} = \frac{\partial \mathcal{H}}{\partial J}, \quad \frac{dJ}{dt} = -\frac{\partial \mathcal{H}}{\partial \theta}, \qquad (9)$$

with Hamiltonian

$$\mathcal{H} = \sum_{j=1}^{N}\left[\frac{1}{2\Gamma_j}p_j^2 - 2\Gamma_j\sqrt{\frac{J}{N}}\cos(x_j-\theta)\right] - \Omega J. \qquad (10)$$

From Eq. (10) it is clear that the SWM model consists of N *pendulum Hamiltonians* mean-fieldcoupled through the amplitude J and the phase θ. Therefore, as the standard map is the symplectic discretization of the pendulum Hamiltonian, the models studied here will consist of an ensemble of N standard maps. In the absence of coupling, i.e., ignoring self-consistency, J and θ would be constant and the parameters of the standard map would be fixed numbers. However, when self-consistency is incorporated, J and θ become dynamical variables (also described by symplectic maps), and this leads to a dependence of the parameters of the maps on $\{x_1,x_2,\ldots,x_N\}$ which gives rise to a global coupling of the maps. The specific form of this coupling will be discussed in Sec. III, where we present a systematic discussion of the map models in terms of generating functions.

The remaining of this paper is organized as follows. In Sec. II we briefly review the diffusion properties in the case of the passive scalar, with particular emphasis on the standard map. As mentioned before, in Sec. III we introduce the two self-consistent systems studied in this work. Sections IV and V are devoted to the discussion of the numerical results. Section VI contains the conclusions.

II. A BRIEF REVIEW OF THE DIFFUSION PROPERTIES OF PASSIVE SCALARS

There exists a huge literature about the transport properties in the passive scalar limit [1,2,17]. On the contrary, there are very few attempts in the study of the self-consistent diffusion. The aim of this section is to recall the main results on the diffusion problem for passive scalars in order to compare

them with the self-consistent diffusion that will be considered in the following sections. It is remarkable that the Lagrangian motion can exhibit nontrivial behavior even for a very simple velocity field $\mathbf{v}(\mathbf{x},t)$ [17,18]. Complex behavior can be originated both from chaotic advection (which is in general possible for stationary $3d$ flows or for time-dependent $2d$ flows) and/or from combined effects of the molecular diffusivity and the advection velocity. Under very general conditions (see below) the large scale field $\langle\Theta\rangle$, which is obtained as an average of a field Θ evolving through Eq. (1) on a volume whose dimensions are much larger than the typical length scale of $\mathbf{v}$, obeys at large times a diffusion equation

$$\frac{\partial\langle\Theta\rangle}{\partial t}=\sum_{i,j}D_{ij}^{E}\frac{\partial^{2}\langle\Theta\rangle}{\partial x_{i}\partial x_{j}},\qquad(11)$$

with eddy diffusivity D_{ij}^{E}. In other words, the effect of the velocity field at large scales and time is the renormalization of the transport coefficient D_{0}. It is easy to understand the origin of Eq. (11) in the Lagrangian framework. Starting from Eq. (4), taking the average over many tracers, one has

$$\langle(x_{i}(t)-x_{i}(0))^{2}\rangle=2D_{0}t+\int_{0}^{t}\int_{0}^{t}dt_{1}dt_{2}\langle v_{i}(\mathbf{x}(t))v_{i}(\mathbf{x}(t))\rangle$$

$$=2D_{0}t+2\int_{0}^{t}dt_{2}\int_{0}^{t_{2}}dt_{1}C_{ii}(t_{2}-t_{1}),\quad(12)$$

where we have assumed that $\langle v_{i}(\mathbf{x}(t))\rangle=0$ and we have introduced the correlation of Lagrangian velocities $C_{ij}(t)\equiv\langle v_{i}(\mathbf{x}(t))v_{j}(\mathbf{x}(0))\rangle$. At large times, if the correlation decays sufficiently fast, the integral in Eq. (12) converges to an asymptotic value

$$\int_{0}^{\infty}dt\,C_{ii}(t)=\langle v_{i}^{2}\rangle T_{L},\qquad(13)$$

which defines the Lagrangian correlation time T_{L}. From Eq. (12) one recovers the Taylor result [19]

$$\langle(x_{i}(t)-x_{i}(0))^{2}\rangle\approx 2(D_{0}+\langle v_{i}^{2}\rangle T_{L})t\equiv 2D_{ii}^{E}t,\qquad(14)$$

which defines the eddy diffusivity in Eq. (11).

Beyond the above typical scenario one can have anomalous dispersion, i.e.,

$$\langle(x_{i}(t)-x_{i}(0))^{2}\rangle\sim t^{2\nu}\qquad(15)$$

with $\nu\neq 1/2$. The case $\nu<1/2$ is called subdiffusion. Superdiffusion ($\nu>1/2$) has been observed in incompressible flows [21], random shear flows and, as we will see, also symplectic maps [20,22]. Anomalous diffusion can occur only if some of the hypothesis of the above argument breaks down. Practically, this can be due to two different mechanisms: (a) infinite variance of the velocity, $\langle v^{2}\rangle=\infty$. (b) Lack of decorrelation, $T_{L}=\infty$.

The first condition, which leads to the class of Lévy flights, is not particularly realistic in physical systems, because it requires infinite energy. We will not discuss here this

behavior. Case (b) is physically more relevant. From Eq. (13) one sees that anomalous superdiffusion is possible only if $C_{ii}(t)$ goes to zero slower than t^{-1}. Unfortunately, the behavior of $C_{ij}(t)$ is generated by the Lagrangian dynamics itself so it is not trivial at all, in the absence of molecular diffusivity, to determine whether the diffusion process will be standard or anomalous. If molecular diffusivity is present rather general results due to Avellaneda, Majda, and Vergassola [23] show that, if the infrared contributions to $\mathbf{v}(\mathbf{x},t)$ are not too strong, standard diffusion occurs.

Let us now discuss the well-known results for the diffusive behavior of the standard map (a complete overview can be found in Ref. [22]),

$$x(t+1)=x(t)+y(t+1)\qquad\text{mod }2\pi,\qquad(16)$$

$$y(t+1)=y(t)+K\sin(x(t)).\qquad(17)$$

The Taylor argument, when applied to the $y(t)$ component [in this work we always refer to the diffusion properties of $y(t)$] of the standard map gives

$$D_{y}^{E}(K)=\frac{1}{2}K^{2}\langle\sin^{2}x\rangle+\sum_{t=1}^{\infty}K^{2}\langle\sin x(t)\sin x(0)\rangle.\quad(18)$$

At large K, the map Eqs. (16) and (17) exhibits widespread stochasticity and to a good approximation consecutive angles x are decorrelated, thus one can neglect the second term in Eq. (18) to obtain the quasilinear (or random phase approximation, RPA) result [22]:

$$D_{y}^{E}(K\gg 1)\approx D_{QL}=\frac{K^{2}}{4}.\qquad(19)$$

The above estimate is very crude: indeed it provides a good estimation of the diffusion coefficient only at very high K. Higher order corrections to the RPA approximation can be obtained by means of the Fourier technique [22]. At order $K^{-1/2}$ one obtains

$$D_{y}^{E}(K)=\frac{K^{2}}{4}\left[1-\sqrt{\frac{8}{\pi K}}\cos\left(K-\frac{5\pi}{4}\right)\right].\qquad(20)$$

This approximation is rather good apart from small K and around *particular* values of K. For $K\lesssim K_{c}\approx 0.972$ because of the presence of separating KAM tori there is not diffusion at all, $D_{y}^{E}(K)=0$. On the other hand, at specific values of K (e.g., $K\approx 6.9115$) corresponding to the existence of ballistic solutions in the y direction, instead of the standard diffusion one observes an anomalous transport with $\nu>1/2$ [24].

III. SELF-CONSISTENT MAP MODELS

In this section we introduce the symplectic map models that we propose for studying diffusion in self-consistent systems. As discussed in Sec. I, these maps consists of ensembles of globally coupled standard maps.

The definition of the maps and the coupling is guided by the well-known fact that if $(\mathbf{q},\mathbf{p})$ denotes the canonical conjugate coordinates of a Hamiltonian system at time n, then

the transformation $(\mathbf{q},\mathbf{p})\rightarrow(\mathbf{q}',\mathbf{p}')$ given by

$$\mathbf{q}'=\frac{\partial S}{\partial \mathbf{p}'}, \quad \mathbf{p}=\frac{\partial S}{\partial \mathbf{q}} \tag{21}$$

defines a symplectic map with generating function $S=S(\mathbf{q},\mathbf{p}')$ [22].

The generating functions of the models proposed here have the generic form

$$S=S_p+S_f+S_i, \tag{22}$$

where S_p defines the uncoupled evolution of the particles, S_f defines the uncoupled evolution of the mean field, and S_i defines the particles-mean-field interaction.

For S_p we assume the standard map generating function

$$S_p=\sum_{n=1}^{N}\left(x_ny_n'+\frac{1}{2\Gamma_n}y_n'^2+K_n\cos x_n\right), \tag{23}$$

where Γ_n, and K_n are constants, the index n labels the particles, and we have used the notation $x(t)=x$ and $x(t+1)=x'$. In S_p the particles are uncoupled and each one follows independently a standard map dynamics.

In order to preserve the symplectic structure of the system, the field is represented by two conjugate variables a phase θ and an amplitude J which, in the absence of interaction with particles, evolve according to the generating function

$$S_f=\theta J'+\int \omega(\bar{J}')d\bar{J}', \tag{24}$$

according to which

$$\theta'=\theta+\omega(J'),$$

$$J'=J. \tag{25}$$

That is, in the absence of coupling the amplitude and frequency of the mean field are constant.

The self-consistent coupling between the particles and the mean field is specified by two functions f and g in the interaction generating function

$$S_i=g(J')\sum_{n=1}^{N}f(x_n-\theta). \tag{26}$$

Based on this generating function, we will consider two models, one introducing a coupling only through the phase of the mean field, and another introducing a coupling through the phase and the amplitude of the mean field.

A. Phase coupling

In this case, it is assumed that

$$g=\varepsilon, \quad f=\sin(x_n-\theta), \quad \omega=\Omega J', \tag{27}$$

and $\Gamma_n=1$, $K_n=K$ for $n=1,2,\ldots,N$; with ε, Ω, K constants. The complete equations of motion thus become

$$x_n'=x_n+y_n' \quad \text{mod } 2\pi,$$

$$y_n'=y_n+K\sin x_n+\varepsilon\cos(x_n-\theta),$$

$$\theta'=\theta+\Omega J',$$

$$J'=J-\varepsilon\sum_{n}\cos(x_n-\theta). \tag{28}$$

The parameter ε measures the strength of the coupling. For $\varepsilon=0$ we recover the situation discussed in the preceding section for N independent particles. One may expect that, in general, the inclusion of a coupling between the different particles will change the diffusive behavior of the system. If there were no feedback from the particle variables x_n to the field J (i.e., no self-consistency) one could argue that the effect of the field variable θ in Eqs. (28) would be the same as that of a noise and thus will destroy the correlations in the y_n variables. In this case one expects that the deviations of the diffusion coefficient with respect to the quasilinear prediction discussed in the preceding section would be strongly suppressed. Of course, this kind of argument cannot be completely justified in presence of the full coupling in Eqs. (28).

B. Amplitude and phase coupling

In this second case, it is assumed that

$$g=2\sqrt{J'}, \quad f=\Gamma_n\cos(x_n-\theta), \quad \omega=-\Omega, \tag{29}$$

where Ω is constant and Γ_n are N independent parameters. The dynamics in this case is determined by

$$x_n'=x_n+y_n'/\Gamma_n,$$

$$y_n'=y_n+K\sin x_n-2\Gamma_n\sqrt{J'}\sin(x_n-\theta),$$

$$\theta'=\theta-\Omega-\frac{1}{\sqrt{J'}}\sum_{n=1}^{N}\Gamma_n\cos(x_n-\theta),$$

$$J'=J+2\sqrt{J'}\sum_{n=1}^{N}\Gamma_n\sin(x_n-\theta), \tag{30}$$

where, to simplify matters, we have assumed that the external field is such that $K_n/\Gamma_n=K$ being K a constant. This globally coupled map was originally proposed in Ref. [10] as a symplectic discretization of the single wave model Hamiltonian system in Eq. (10). Compared with Eq. (28), in the map (30) J and θ are both coupled to the particles and this leads to a self-consistent modification of the phase *and* the amplitude of the mean field.

The map for J is implicit. However, rescaling the variables $y_n\rightarrow\Gamma_ny_n$, $K\rightarrow\Gamma_nK$, and defining

$$\kappa=2\sqrt{J}, \quad \gamma_n=2\Gamma_n, \quad \eta=\sum_{n=1}^{N}\gamma_n\sin(x_n-\theta), \tag{31}$$

the map can be written in a fully explicit form as [10]

$$x'_n = x_n + y'_n,$$

$$y'_n = y_n + K \sin x_n - \kappa' \sin(x_n - \theta),$$

$$\kappa' = \sqrt{\kappa^2 + \eta^2} + \eta,$$

$$\theta' = \theta - \Omega + \frac{1}{\kappa'} \frac{\partial \eta}{\partial \theta}. \tag{32}$$

In this model, the mean-field amplitude κ plays the role of the standard map parameter (besides the K constant), which is self-consistently coupled to the particles through the order parameter η. In the mean-field particle dynamics one can define the total *momentum* of the system as

$$\mathcal{P} = \frac{\kappa^2}{2} + \sum_{n=1}^{N} \gamma_n y_n, \tag{33}$$

where the first term on the right hand side represents the momentum of the mean field, and the second term the total momentum of the particles. This quantity is a constant of motion of Eq. (30),

$$\mathcal{P}' = \mathcal{P}. \tag{34}$$

This conservation law plays an important role in the diffusive properties of the system.

IV. DIFFUSION IN PHASE COUPLED MAPS

Let us study the diffusion properties in the phase coupled map (28). In particular, we will see that the effect of the mean-field coupling is the randomization of the phase. That is, when coupling occurs only through the phase, self-consistency increases the stochasticity of the map, and the diffusive properties of the coupled maps are practically indistinguishable from the dynamics of a phase-randomized uncoupled map.

In the limit $\varepsilon = 0$ the diffusion coefficient (for the y component), as a function of the parameter K, displays the complex behavior discussed in Sec. II. The first natural question is whether this complexity survives in the presence of coupling with a self-consistent mean field (i.e., for $\varepsilon > 0$).

In Fig. 1 we show $D_y^E(K)$ (normalized with the RPA prediction $K^2/4$) in the uncoupled case ($\varepsilon = 0$) and for some other values of the coupling ($\varepsilon = 0.05$ and $\varepsilon = 0.1$). Numerically, $D_y^E(K)$ is calculated by taking the large time limit of the expression

$$D_y^E(t) = \frac{\langle [y(t) - y(0)]^2 \rangle}{2t}. \tag{35}$$

For comparisons, we also plot the value of $D_y^E(K)/D_{QL}$ with the higher order RPA corrections as given by Eq. (20). As one can see, for a generic large value of K the presence of a small coupling do not change the diffusion coefficient, apart for the values at which one can observe anomalous diffusion
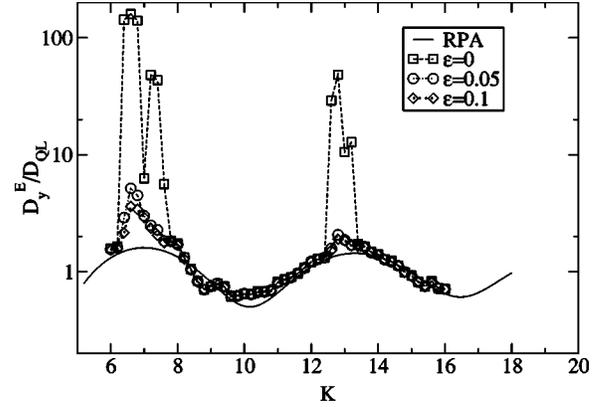

FIG. 1. Normalized diffusion coefficient vs K for different values of the ε parameter; squares for $\varepsilon = 0$, circles $\varepsilon = 0.05$ and diamonds for $\varepsilon = 0.1$. Solid line represents the theoretical prediction as given by the higher order RPA approximation (20). The number of particles is $N = 60\,000$, $\Omega = 0.1$ and the number of steps is 10 000.

in the uncoupled limit ($\varepsilon = 0$). Therefore, the first effect of the mean field is to remove the ballistic contributions to the dispersion.

Thus, let us try to focus on the case, where the standard map ($\varepsilon = 0$) shows an anomalous behavior, for e.g., $K = 6.9115$, and see where the differences with the self-consistent map ($\varepsilon \neq 0$) appear. The diffusion coefficient is an asymptotic quantity. For finite time, the evolution of Eq. (28) with small ε maintains a memory of the behavior at $\varepsilon = 0$ up to a time $T(\varepsilon)$ (saturation time). We define $T(\varepsilon)$ as the time at which the finite-time diffusion coefficient, as given by Eq. (35), is reasonably close to its asymptotic value.

In Fig. 2 we show $T(\varepsilon)$, for a system with $K = 6.9115$, as a function of $1/\sqrt{\varepsilon}$. The approximately linear behavior in the plot indicates the dependence $T(\varepsilon) \sim \exp(c/\sqrt{\varepsilon})$, with c an arbitrary constant. Let us note that the anomalous diffusion is mainly due to the presence of ballistic (nonchaotic) trajectories. Therefore, the failing of anomalous transport can be seen as the recover of a generic statistical behavior. In this sense this is consistent with a scenario *á la Nekhoroshev* [22]. We also remark that, within the range of values investigated, there is not evidence of dependence on the size N as
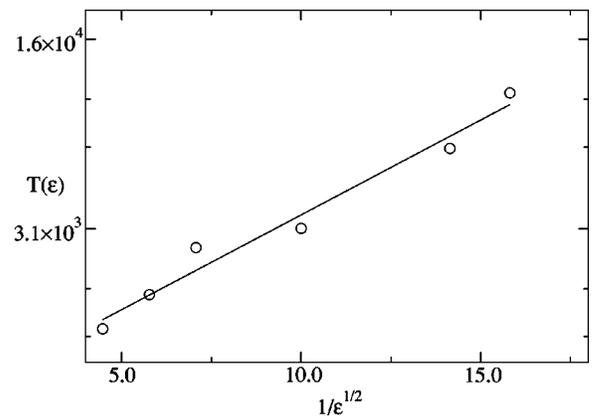

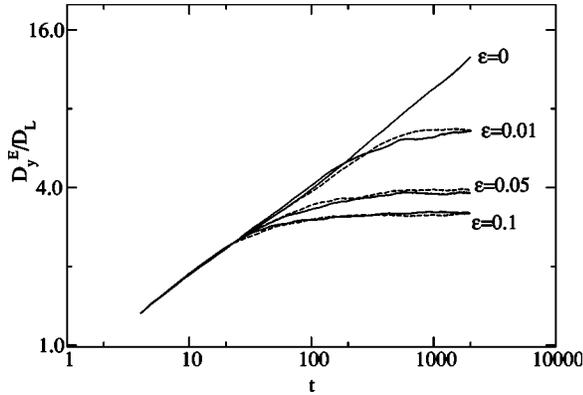FIG. 2. Saturation time, $T(\varepsilon)$, vs $1/\sqrt{\varepsilon}$ for $K = 6.9115$ and $N = 60\,000$.

FIG. 3. D_y^E/D_{QL} against time for two different number of particles, $K=6.9115$, and different values of ε. Solid line is for $N=60\,000$ and the dashed line for $N=40\,000$.

FIG. 4. $D_y^E(K=6.9115)/D_{QL}$ vs time for different values of ε and $N=60\,000$. The solid line is for an external self-consistent field and the dashed line is for an external random field. The random external field is generated by picking, at every time step, a random number regularly distributed in the interval $[0,2\pi]$.

can be seen in Fig. 3 (again for $K=6.9115$). It is worth mentioning here that in Fig. 3 for $\varepsilon=0$ one observes the typical anomalous behavior of the diffusivity, that is, $D_y^E \propto t^{0.3}$ [24].

The discussed results indicate that the main effect of the self-consistent field is to reduce the deviations from the statistical prediction. This is to be expected because in this case, as mentioned before, the phase coupling leads to a randomization of the phase which is precisely what is assumed in the statistical arguments based on the random phase approximation. We check this statement by replacing the self-consistent field with an external noise. We study a system of N particles whose evolution is now given by a time-dependent generating function

$$S(\{x'_n\},\{y_n\},t)=\sum_{n=1}^{N} S_0(x'_n,y_n)+\varepsilon\sum_{n=1}^{N} f(x'_n-\eta(t)),$$

(36)

where η is a random process with the same statistical properties of the self-consistent θ, i.e., η is a random number uniformly distributed in the interval $[0,2\pi]$. The result for $D_y^E(K=6.9115)/D_{QL}$ against time is plotted in Fig. 4 for both the self-consistent and the random field. One observes that the random approximation is rather accurate. Therefore, taking into account the results for K large and the specific values of K, where the standard map is anomalous, one can say that the dynamics for K large in the self-consistent map model (28) is equivalent to an *effective* standard map.

Most interesting, *a priori*, is the case of small values of K. As we have recalled in the preceding section, for $K<1$ and $\varepsilon=0$ there is no diffusion due to the presence of KAM tori. However, as Fig. 5 shows, the phase coupled ($\varepsilon \neq 0$) self-consistent map displays finite diffusion for arbitrary small values of K. This is, once again, a manifestation of self-consistent driven phase randomization.

The same scenario as for large values of K has been identified, that is, the external self-consistent field is equivalent, when diffusion properties are under study, to an external random field. This can be seen again in Fig. 5, where we also plot the diffusion coefficient obtained from the effective ran-
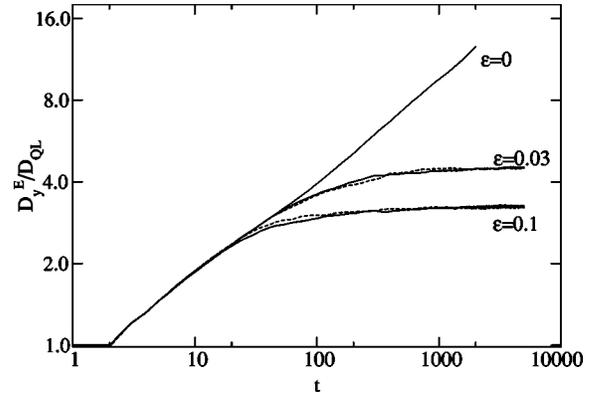
dom map. At small K, one observes a weak dependence of D_y^E on K, while $D_y^E \simeq \varepsilon^2/4$, leading to a finite diffusivity also for $K=0$. As mentioned before, it is the breaking of the regular orbits of the standard map (for K small) induced by the mean field, that allows the diffusion of particles. This is clearly seen in Fig. 6 where it is shown some trajectories in the phase space for $K=1$ for both the standard map and the coupled map model (28) with $\varepsilon=0.1$.

In summary, for model (28) the coupling to an external self-consistent mean field is equivalent to the effect induced by an external random field. This result is valid also for $K<1$, where the standard map shows barriers to transport.

V. DIFFUSION IN FULLY SELF-CONSISTENT MAPS

In this section we study the diffusive properties of fully self-consistent maps. By this we mean maps coupled through the phase *and* the amplitude of the mean field. Our study will be based on map (32) with $\Omega=0$, and in the absence of
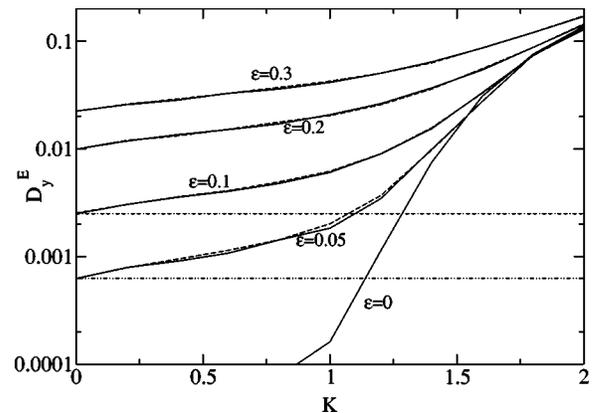

FIG. 5. D_y^E vs K for different values of ε. Here the number of particles is $N=60\,000$ and the final time is 10 000. The solid line is for an external self-consistent field and the dashed line is for an external random field. The straight lines correspond to the lines $D_y^E=\varepsilon^2/4$ for $\varepsilon=0.1$ (dashed-dotted) and $\varepsilon=0.05$ (dashed-doubledotted).
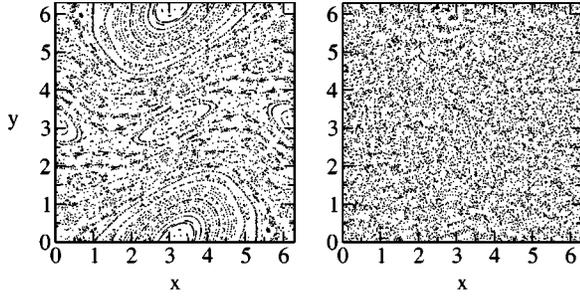
FIG. 6. Left, standard map phase space for $K=1$, and, right, the trajectory of one particle for the system Eq. (28) with $K=1$ and $\varepsilon=0.1$.

external field ($K=0$) since we are mostly interested in self-consistent effects.

We consider an ensemble of N particles with coordinates (x_j, y_j), $j=1,2,\ldots,N$, in the rectangle $x \in (-\pi, \pi)$ and $y \in (-\pi/2, \pi/2)$. We will focus in the study of a Gaussian distributed active field

$$\gamma_j = \gamma_0 \exp\left[\frac{-(x_j^2 + y_j^2)}{2\sigma^2}\right]. \tag{37}$$

For these nonuniform γ_j distributions it is useful to distinguish between the particle variance σ_{py}^2, and the concentration variance $\sigma_{\gamma y}^2$ defined as

$$\sigma_{py}^2 = \langle[y-\langle y \rangle_p]^2\rangle_p, \quad \sigma_{\gamma y}^2 = \langle[y-\langle y \rangle_\gamma]^2\rangle_\gamma, \tag{38}$$

where

$$\langle q \rangle_p = \frac{1}{N}\sum_{j=1}^{N} q_j, \quad \langle q \rangle_\gamma = \frac{1}{N}\sum_{j=1}^{N} \gamma_j q_j. \tag{39}$$

A. Subcritical diffusion

In the first simulation we iterated the map with initial conditions $\kappa(1)=0.8$, and $\theta(1)=0$. The upper panel of Fig. 7 shows the initial γ distribution. For $t>0$, the scalar mixes and in the process modifies κ and θ. In particular, in this case, as shown in Fig. 8, κ oscillates in time around a mean value $\langle\kappa\rangle=0.966$ ($\langle\cdot\rangle$ is the temporal average) slightly below the critical value $\kappa_c=0.9716$ for the destruction of KAM barriers and the onset of diffusion in the standard map. The phase (see also Fig. 8) decreases monotonically.

That is, the self-consistent coupling drives the system periodically between a diffusive regime with no KAM barriers ($\kappa > \kappa_c$) and a nondiffusive regime with KAM barriers ($\kappa < \kappa-c$). As shown in Fig. 9, this yields to diffusive particle transport in y, $\sigma_{py}^2 = 2Dt$, even though on the average κ is below the threshold for diffusion, that is there is subcritical diffusion. Because the peak of the γ distribution remains coherent, in this case there is no diffusion in the concentration. As discussed in the preceding section, also in phase coupled map (28) there is a subcritical diffusion regime. However, there is an important difference between these two cases because in the phase coupled map the time evolution of
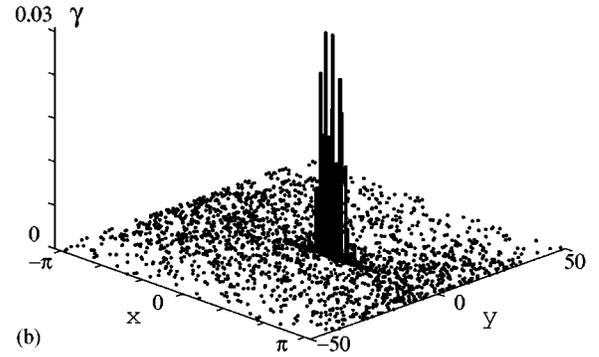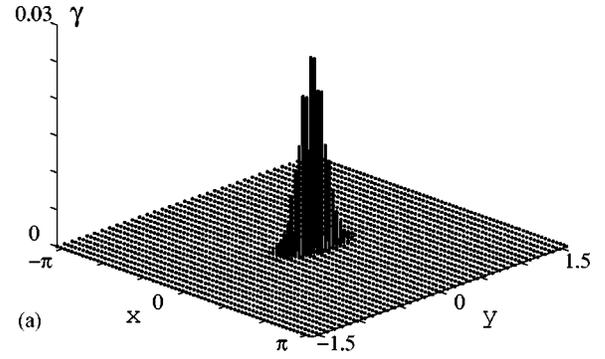

FIG. 7. Phase space particle distribution in the fully self-consistent map (32) for a Gaussian distributed active scalar according to Eq. (37) with $2\sigma^2=0.2$ and $\gamma_0=0.0269$ and initial conditions $\kappa(1)=0.8$ and $\theta(1)=0$. The two panels show the particle distribution at the initial and final time, after 137 000 steps. The height of a vertical lines corresponds to the active scalar concentration γ_j of the jth particle located at $(x,y)=(x_j, y_j)$.

the phase θ exhibits random behavior while in the fully self-consistent map, as shown in Fig. 8, θ has a regular behavior.

The oscillations of κ are caused by the feedback effect of the active scalar trapped in the period-one island of the map (see Fig. 7). We describe the coherent part of the distribution, i.e., the part of the distribution trapped in the period-one island, as a *macroparticle*. The macroparticle representation is a sort of renormalization process in which a group of particles with different values of γ_k are replaced by one with an effective γ. The macroparticle concept provides a link between systems with large (or infinite) degrees of freedom and low dimensional systems [16,12,25]. In the case considered here, at a given time t, the macroparticle rotates around the o point of an effective standard map with coupling constant $K=\kappa(t)$ and phase $\theta(t)$.

The oscillation period for a standard map of coupling parameter K can be estimated as [22]

$$T = \frac{2\pi}{\arccos\left(1 - \dfrac{K}{2}\right)}. \tag{40}$$
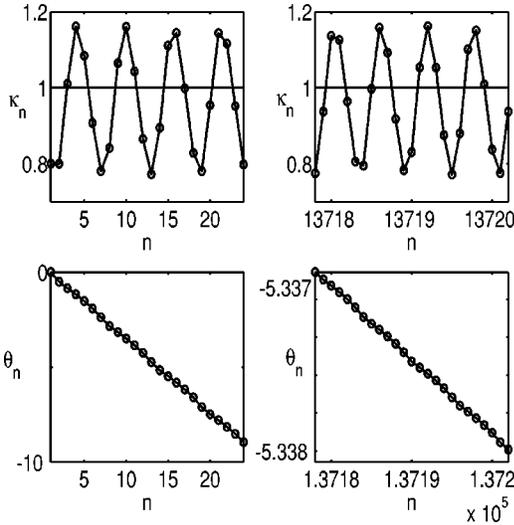
To use this result to calculate the rotation period of the

FIG. 8. Time evolution of κ and θ in fully self-consistent map (32) for a Gaussian distributed active scalar according to Eq. (37) and initial conditions $\kappa(1)=0.8$ and $\theta(1)=0$. The plots show the evolution in time windows at the beginning $n \in (0,60)$ and at the end $n \in (137\,000,137\,060)$ of the run. The same periodic behavior is observed at intermediate times.

self-consistent oscillation of κ, note that according to the conservation of momentum in Eq. (33),

$$\kappa^2(t)=\kappa^2(1)+\sum_{n=1}^{N} \gamma_n[y_n(1)-y_n(t)]. \qquad (41)$$

In the macroparticle description, this relation can be written as

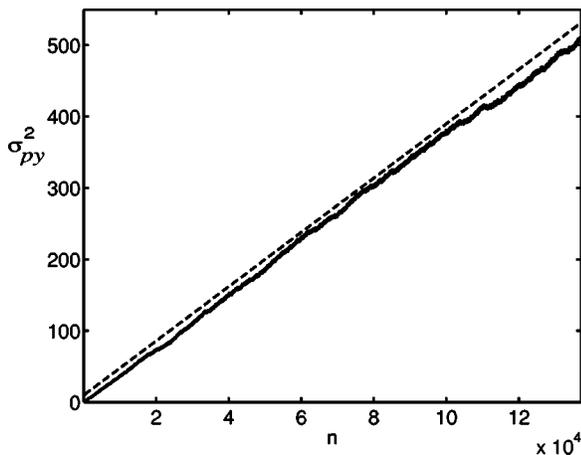$$\kappa^2(t)=\kappa^2(1)+\Gamma_{mc}Y_{mc}(t), \qquad (42)$$

FIG. 9. Subcritical diffusion in fully self-consistent map (32) for a Gaussian distributed active scalar according to Eq. (37) and initial conditions $\kappa(1)=0.8$ and $\theta(1)=0$. Even though in this case, as shown in Fig. 8, the mean value of $\langle \kappa \rangle$ is below the critical value for the destruction of all KAM barriers, the variance shows clear evidence of diffusive transport with $2D_y^E=0.0038$.
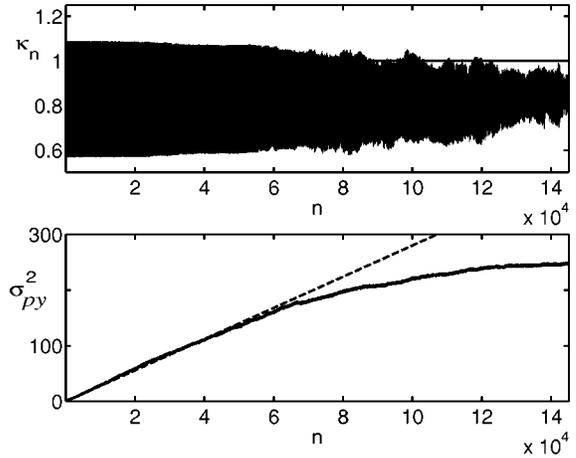

FIG. 10. Self-consistent suppression of diffusion in map (32) for a Gaussian distributed active scalar according to Eq. (37) and initial conditions $\kappa(1)=0.6$ and $\theta(1)=0$. Upper panel shows the time evolution of κ and the lower panel the time evolution of the square of the particle variance. For $n \in (1,6\times10^4)$, κ reaches values above the threshold for KAM barriers destruction ($\kappa_c\approx1$). For later times, the maximum of κ drops systematically below κ_c and diffusion is suppressed.

where $\Gamma_{mc}=\Sigma_n\gamma_n$ is the effective γ_{eff} of the macroparticle and Y_{mc} the y coordinate of the macroparticle. According to Eq. (42), the oscillation period of κ equals the rotation period of the macroparticle, which can be estimated using Eq. (40) with $K=\langle \kappa \rangle$. For $\langle \kappa \rangle \approx 1$ this approximation gives a period $T\approx6$, which is in good agreement with the numerical results (see Fig. 8).

B. Self-consistent suppression of diffusion

In the previous example, the constant rotation of the active scalar trapped in the period-one island gave rise to stationary oscillations of κ and steady particle diffusion in y. However, this is not always the case, and it is possible that diffusion is suppressed rather than maintained by self-consistent effects. As an example, consider the same initial conditions as before but with a smaller initial value of the coupling parameter κ, namely, $\kappa(1)=0.6$. In this case, as Fig. 10 shows, there is an initial regime in which κ oscillates beyond κ_c and diffusive transport is present with $D=0.0014$. However, after a fraction of particles have migrated to regions of large y, κ drops systematically below κ_c and diffusion is suppressed. At this point the system enters in a transient subdiffusive regime leading to the eventual elimination of the diffusion. As shown in Fig. 10, and in more detail in Fig. 11, the suppression of the diffusion is accompanied by a damping of the coupling parameter κ. Note that consistent with the estimation in Eq. (40), the period of oscillation remains constant $T\approx6$. According to momentum conservation in Eq. (42), this damping can be viewed as a momentum transfer from the mean field to the particles. This is reminiscent of the Landau damping mechanism in plasmas in which an energy transfer from the field to the particles leads to a collisionless damping of the field.
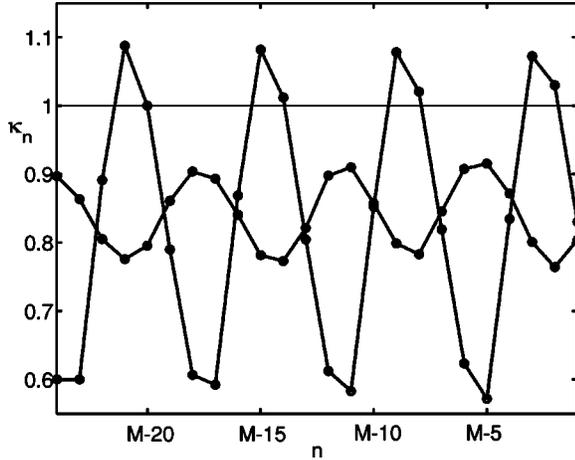
FIG. 11. Damping of κ during the self-consistent suppression of diffusion shown in Fig. 10. The curve with larger amplitude shows the beginning of the time series (top panel of Fig. 10 with $M = 25$) and the curve with the smaller amplitude shows the tail of the time series (top panel of Fig. 10 with $M = 14 \times 10^4$).

C. Macroparticle instability and diffusion of concentration

In the previous examples, the value of κ was relatively small, and the macroparticle (i.e., the conglomerate of particles with the largest values of γ) remained coherent. This yields either steady diffusion (see Fig. 9) or transient diffusion (see Fig. 10) of the particle distribution, but no diffusion of the concentration, i.e., $\sigma_{\gamma y} \approx 0$. However, self-consistent effects can destabilize the macroparticle and the concentration field diffuses. To illustrate this, we consider the same Gaussian distribution [Eq. (37) as before but with a larger initial value of κ, namely, $\kappa(1) = 3.3$]. In this case, as Fig. 12 shows, up to $n \approx 5 \times 10^3$, κ remains approximately constant, the phase θ_n [panel (b)] decreases monotonically, the concentration variance $\sigma_{\gamma y}$ does not grow and the particle variance σ_{py} exhibits standard diffusion. Around $n \approx 5 \times 10^3$ there is a transition and κ grows rapidly giving rise to a diffusion of the concentration and a jump in the particle diffusion. Figure 13 shows the active scalar distribution at two different times.

D. Quasilinear diffusion

In the phase and amplitude coupled map there is also a regime in which the phase is random and the map is equivalent to a random standard map. This leads to quasilinear diffusion as shown in the following. This regime is approached for initial $\kappa(1)$ such that, in the long-time limit, the time average value $K_{eff} = 1/(N_t - N_0)\Sigma_{n=N_0}^{N_t} \kappa(n)$ is larger than 1, being N_t the final time, and N_0 a proper time chosen to avoid the initial transient behavior. Since the value of κ depends on the iteration time, the eddy diffusivity is also time dependent, and we must define an effective diffusivity, which is nothing but the time average of the instantaneous diffusion, $D_{eff} = 1/(N_t - N_0)\Sigma_{n=N_0}^{N_t} D_y^E(n)$. With these definitions, the quasilinear approximation is recovered. This can
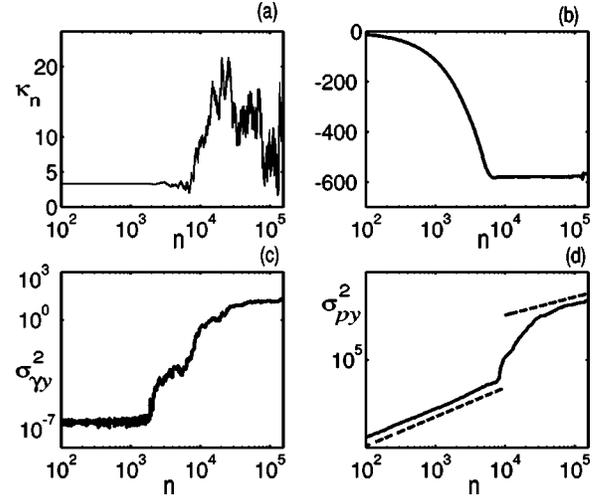

FIG. 12. Macroparticle instability and diffusion of passive scalar concentration in the fully self-consistent map (32) for a Gaussian distributed active scalar according to Eq. (37) and initial conditions $\kappa(1) = 3.3$ and $\theta(1) = 0$. Panel (a) shows the time series of κ_n, (b) the phase θ_n, (c) f the concentration variance $\sigma_{\gamma y}^2$, and (d) the particle variance σ_{py}^2. The lower and upper dashed lines have slopes equal to 1 and 0.62, respectively. Around $n \approx 5 \times 10^3$, the macroparticle looses coherence, κ_n exhibits large fluctuations, θ_n drops to a constant value, and there is a jump in $\sigma_{\gamma y}^2$ and σ_{py}^2.

be seen in Fig. 14 by plotting the D_{eff}/D_{QL} vs K_{eff}, and with solid line we plot the RPA approximation Eq. (20).

VI. CONCLUSIONS

We have studied self-consistent diffusion in active system described by globally coupled symplectic maps. We focused our analysis in two systems: an ensemble of phase coupled maps, and an ensemble of maps coupled through the phase and the amplitude. The latter model is a symplectic discretization of the single wave model and as such represents a simplified description of self-consistent transport in plasmas and fluids. Numerical results obtained with this model indicate that self-consistency plays a critical role in the diffusive properties of the system. In particular, (a) for small initial values of the standard map parameter, $\kappa(1) = 0.8$, coherent oscillations of the active scalar give rise to periodic oscilations of κ above and below the threshold for barrier destruction ($\kappa_c = 0.9716$) leading to subcritical diffusion; (b) for smaller initial values, $\kappa(1) = 0.6$, there is a diffusive transient that eventually is suppressed by self-consistent effects; (c) for larger values, $\kappa(1) = 3.3$, the active scalar loses coherence and this leads to a jump in the particle diffusion and to the diffusion of the concentration field; (d) for large enough initial values of κ there is widespread chaos and (with the exception of initial values close to accelerator models) self-consistency is shadowed by stochasticity leading to quasilinear difusion. The behavior of the phase coupled map is in general different. In this case, we have shown that (a) in the limit of large K, that is strong stochasticity of the flow, the external self-consistent field (at least for diffusion properties) is equivalent to a random field; (b) the singular properties of the standard map, like the existence of ballistic
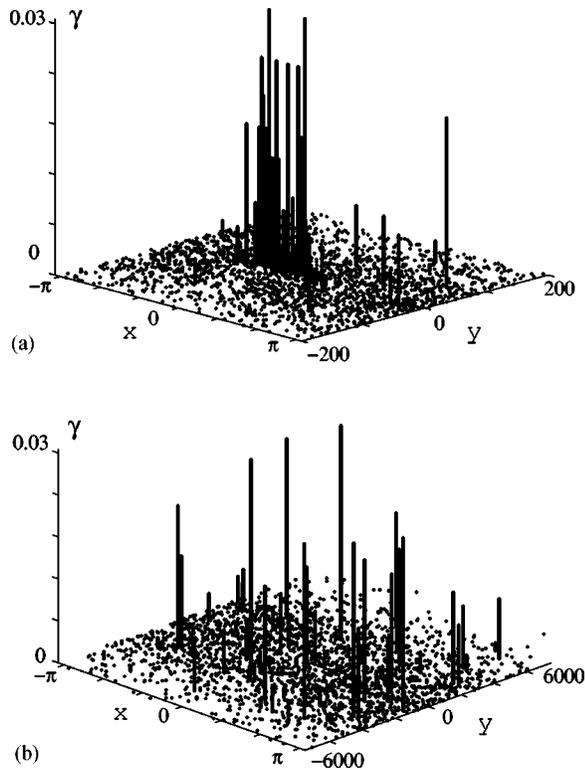
FIG. 13. Active scalar distribution during the macroparticle instability phase [panel (a)], and the diffusive phase [panel (b)] in the fully self-consistent map (32) for the run shown in Fig. 12. The initial condition corresponds to the Gaussian distributed profile in Eq. (37) shown in Fig. 7. In the plots, the height of a vertical line centered at (x,y) corresponds to the active scalar concentration γ_j of the jth particle located at $(x,y)=(x_j,y_j)$.

modes giving rise to anomalous diffusion, are overcome by the external field; (c) for K small, diffusion is different from zero, i.e., the external field breaks the barriers to transport present in the standard map. Moreover, again the external field is equivalent to a random driving field.
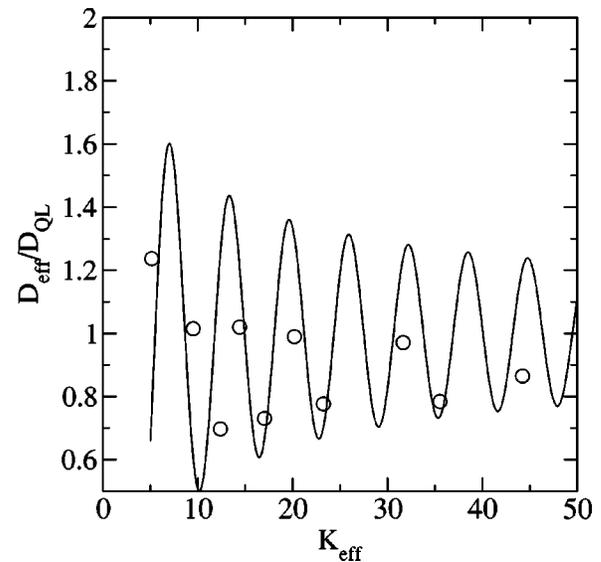

FIG. 14. With circles the numerically obtained values for D_{eff}/D_{QL} against K_{eff}. Solid line shows the RPA approximation Eq. (20).

[1] H.K. Moffatt, Rep. Prog. Phys. **46**, 621 (1983).

[2] J. M. Ottino, *The Kinematics of Mixing: Stretching, Chaos and Transport* (Cambridge Univ. Press, Cambridge, 1989).

[3] J. D. Murray, *Mathematical Biology* (Springer, New York, 1993); J. Xin, SIAM Rev. **42**, 161 (2000).

[4] See for example the *Focus Issue on Active Chaotic Flow*, Chaos **12**, 372 (2000), edited by Z. Toroczkai and T. Tél; E. Hernández-Garcia, C. López, and Z. Neufeld, in *Chaos in Geophysical*, edited by G. Lacorata, G. Boffetta, G. Visconti, and A. Vulpani (in press). Also available in arXiv.org/nlin.CD/0205009.

[5] H. Lamb, *Hydrodynamics* (Dover, New York, 1945).

[6] D. R. Nicholson, *Introduction to Plasma Theory* (Krieger Publishing Co., Florida, 1992).

[7] S. Chandrasekhar, Rev. Mod. Phys. **15**, 1 (1943).

[8] J. Binney and S. Tremaine, *Galactic Dynamics* (Princeton University Press, Princeton, NJ, 1987).

[9] H. Aref, Annu. Rev. Fluid Mech. **15**, 345 (1983).

[10] D. del-Castillo-Negrete, Chaos **10**, 75 (2000).

[11] D. del-Castillo-Negrete, Physica A **280**, 10 (2000).

[12] D. del-Castillo-Negrete and M.-C. Firpo, Chaos **12**, 496 (2002).

[13] T.M. O'Neil, J.H. Winfrey, and J.H. Malmberg, Phys. Fluids **14**, 1204 (1971); H.E. Mynick and A.N. Kaufman, *ibid.* **13**, 2422 (1970); D. del-Castillo-Negrete, Phys. Plasmas **5**, 3886 (1998); M-C. Firpo, F. Doveil, Y. Elskens, P. Bertrand, M. Poleni, and D. Guyomarc'h, Phys. Rev. E **64**, 026407 (2001).

[14] N.J. Balmforth and C. Piccolo, J. Fluid Mech. **449**, 85 (2001).

[15] M. Antoni and S. Ruffo, Phys. Rev. E **52**, 2361 (1995).

[16] J.L. Tennyson, J.D. Meiss, and P.J. Morrison, Physica D **71**, 1 (1994).

[17] T. Bohr, M. Jensen, G. Paladin, and A. Vulpiani, *Dynamical*

Systems Approach to Turbulence (Cambridge University Press, Cambridge, 1998); A. Crisanti, M. Falcioni, G. Paladin, and A. Vulpiani, Riv. Nuovo Cimento **14**, 1 (1991).

[18] H. Aref, J. Fluid Mech. **143**, 1 (1984).

[19] G.I. Taylor, Proc. R. Soc. London, Ser. A **219**, 186 (1953); **225**, 473 (1954).

[20] G.M. Zaslavsky, D. Stevens, and H. Weitzner, Phys. Rev. E **48**, 1683 (1993).

[21] D. del-Castillo-Negrete, Phys. Fluids **10**, 576 (1998).

[22] A. J. Lichtenberg and M. A. Lieberman, *Regular and Chaotic Dynamics*, 2nd ed. (Springer-Verlag, New York, 1992).

[23] M. Avellaneda and A. Majda, Commun. Math. Phys. **138**, 339 (1991); M. Avellaneda and M. Vergassola, Phys. Rev. E **52**, 3249 (1995).

[24] P. Castiglione, A. Mazzino, P. Muratore-Ginanneschi, and A. Vulpiani, Physica D **134**, 75 (1999).

[25] D. del-Castillo-Negrete, in *Dynamics and Thermodynamics of Systems with Long Range Interactions*, Lecture Notes in Physics Vol. 602, edited by T. Dauxois, S. Ruffo, E. Arimondo, and M. Wilkens, (Springer, New York, 2002).